Semiclassical approach to fidelity amplitude

2011 New J. Phys. 13 103040

(http://iopscience.iop.org/1367-2630/13/10/103040)

New Journal of Physics
The open-access journal for physics

Semiclassical approach to fidelity amplitude

Ignacio García-Mata[1,2], **Raúl O Vallejos**[3,5] **and Diego A Wisniacki**[4,5]

[1] Instituto de Investigaciones Físicas de Mar del Plata (IFIMAR), CONICET—UNMdP, Funes 3350, B7602AYL Mar del Plata, Argentina
[2] Consejo Nacional de Investigaciones Científicas y Tecnológicas (CONICET), Argentina
[3] Centro Brasileiro de Pesquisas Físicas (CBPF), Rua Dr Xavier Sigaud 150, 22290-180 Rio de Janeiro, Brazil
[4] Departamento de Física 'J J Giambiagi', FCEN, Universidad de Buenos Aires, 1428 Buenos Aires, Argentina
E-mail: vallejos@cbpf.br and wisniacki@df.uba.ar

New Journal of Physics **13** (2011) 103040 (19pp)
Received 21 June 2011
Published 31 October 2011
Online at http://www.njp.org/
doi:10.1088/1367-2630/13/10/103040

Abstract. The fidelity amplitude (FA) is a quantity of paramount importance in echo-type experiments. We use semiclassical theory to study the average FA for quantum chaotic systems under external perturbation. We explain analytically two extreme cases: the random dynamics limit—attained approximately by strongly chaotic systems—and the random perturbation limit, which shows a Lyapunov decay. Numerical simulations help us to bridge the gap between both the extreme cases.

[5] Authors to whom any correspondence should be addressed.

Contents

1. Introduction

Irreversibility in quantum mechanics cannot be explained in the same way as in classical mechanics. Instead of measuring how difficult it is to invert the individual trajectories, Peres proposed [1] to measure the difficulty of inverting the dynamics as a way of understanding quantum irreversibility. In other words, he proposed to measure how difficult it is to implement a certain Hamiltonian or to *know* the specifics of the dynamics, given that complete isolation is impossible to attain. As a consequence, the fidelity—also known as the Loschmidt echo (LE) [2]—was proposed as a measure of instability of a given Hamiltonian under external perturbations. The LE is commonly defined as

$$M(t) = |O(t)|^2, \tag{1}$$

where

$$O(t) = \langle \psi_0 | \, \mathrm{e}^{\mathrm{i}H_\varepsilon t/\hbar} \, \mathrm{e}^{-\mathrm{i}H_0 t/\hbar} | \psi_0 \rangle \tag{2}$$

is the fidelity amplitude (FA) and H_0 and H_ε differ by a perturbation that is usually taken to be an additive term such as $\varepsilon V(q, p)$, so ε is the perturbation strength. The importance of the LE lies not only in that it can be used to identify quantum chaos but also in that it is a measurable quantity.

There is a vast amount of work attempting to characterize the decay regimes of the LE as universal [2–5]. After a short time transient, chaotic systems decay exponentially. For small perturbation strength—the Fermi golden rule regime—the decay rate depends quadratically on the perturbation strength. For larger perturbation the decay rate is expected to be perturbation independent and given by the largest Lyapunov exponent of the corresponding classical system. For regular systems the behaviour is fundamentally different: for small perturbation strength the decay is Gaussian—which can in fact lead to faster decay than chaotic systems [6, 7]—and for larger values of the perturbation the decay is power law (for reviews see [4, 5]). However, for chaotic systems, recent works [8–12] have reported non-universal oscillatory behaviour in the decay rate of the LE as a function of the perturbation strength. In the way of elucidating the origin of such 'anomalous' behaviour of the LE, one key quantity to understand is the fidelity amplitude (FA). The FA is important in itself for a number of reasons, the most important being that in some of the echo experiments it is in fact the quantity that is measured [13–18].

It is important to remark that in previous works the characterization of decay regimes is done on the average behaviour of the LE. Unlike most papers in the field—with the exception of [19]—in this work we concentrate on the average FA. The fundamental difference to [19] is that we obtain the decay regimes directly of the average FA, not requiring to compute the average fidelity. In order to do so, we use the semiclassical theory known as dephasing representation (DR) [19–21]. We consider two limiting situations and obtain rigorous analytical expressions for the decay rate in both cases. In the first case, we suppose that the dynamics is completely random. For maps on the torus each step is given by drawing two random numbers from a uniform distribution. This corresponds to the limit of infinite Lyapunov exponent. In this limit we obtain an expression for the decay of the FA that is valid for all times—up to the saturation point. In fact it should be observed for very short times for any map—our expression is exact for $t = 1$. As the Lyapunov exponent is increased the random dynamics decay regime is observed for increasingly longer times. We have already presented related results in [22]. The other limiting case presupposes that the perturbation is completely random. That is, after each step of the map the perturbation contributes with a random phase to each trajectory. It shall be seen that this assumption can be justified in the large perturbation strength limit because semiclassical calculations involve complex exponentials of such strengths. In that case—using the DR and transfer matrix theory—we show that the asymptotic decay rate of the FA is controlled by the largest classical Lyapunov exponent λ. In other words, we are capable of predicting analytically the appearance of a Lyapunov regime in the average FA rather than the fidelity itself (i.e. the square of the modulus of the FA).

Even though in a realistic scenario one may not see clearly the appearance of the limiting behaviour, traces of one (or both) of them are usually present. For short times, on average the decay rate is that predicted for random dynamics. This result is valid for longer times as the dynamics becomes effectively more random—i.e. as λ grows. Then, for large perturbations, there is a crossover to an asymptotic regime where the decay rate is $\lambda/2$, independently of the perturbation. The crossover time is strongly perturbation dependent. We exhibit numerical simulations introducing a perturbation model where the amount of randomness can be varied. In this model the decay of the FA is well described by a sum of two terms, each one corresponding to one of the types of limiting behaviour. The relative weight of the terms depend both on λ and on the perturbation (amplitude and, length scale).

This paper is organized as follows. Section 2 gives a brief introduction to the DR. This semiclassical approximation is the basis of two analytically tractable models to be developed in the subsequent sections. The random-dynamics approach, which is valid for large Lyapunov exponents, is described in section 3. Using the baker-map family as a model of chaotic dynamics and employing the transfer matrix method, we argue in section 4 that for large perturbations the asymptotic decay is ruled by the Lyapunov exponent.

Section 5 presents a brief study of mixed regimes, where the decay of the FA is bi-exponential. We show in some numerical examples that the decay rates are still given by the models mentioned above. An empirical expression for the crossover time is found.

We conclude in section 6 with a summary of our results and some final remarks.

2. Semiclassical dephasing representation of the fidelity amplitude

Recently [19–21], the DR was introduced to give a compact and efficient way of computing the FA semiclassically. The derivation of the DR starts by replacing the quantum propagators by

the semiclassical Van Vleck propagator—this is the standard semiclassical approach. The first innovation is to use the initial value representation for the Van Vleck propagator. In this way a full semiclassical—the so-called uniform—expression for $O(t)$ can be obtained. However, this expression is still too difficult to be computed and a further approximation is needed that involves using trajectories of H_ε with slightly different initial conditions but that remain close to the trajectories of H_0 up to a certain time. The validity of this 'dephasing trajectories' argument was justified using the shadowing theorem [19]. One of the forms of the FA obtained using the DR looks like

$$O_{\mathrm{DR}}(t) = \int \mathrm{d}q\, \mathrm{d}p\, W_\psi(q, p) \exp(-\mathrm{i}\Delta S_\varepsilon(q, p, t)/\hbar), \tag{3}$$

where $W(q, p)$ is the Wigner function of the initial state ψ and

$$\Delta S_\varepsilon(q, p, t) = -\varepsilon \int_0^t \mathrm{d}\tau\, V(q(\tau), p(\tau)) \tag{4}$$

is the action difference evaluated along the unperturbed classical trajectory. In this way the decay can be attributed to the dephasing produced by the perturbation of the actions—thus the name DR. However, numerics show that equation (3) also accounts for decay due to classical overlaps [21].

The DR is a useful tool to compute fidelity and to assess fidelity decay. Actually, when referring to fidelity decay *regimes*, one refers to average behaviour. Throughout this work by average we mean average over initial states. The average FA over a number n_r of initial states is

$$\overline{O_{\mathrm{DR}}(t)} = \frac{1}{n_r} \sum_{i=1}^{n_r} \int \mathrm{d}q\, \mathrm{d}p\, W_{\psi_i}(q, p) \exp(-\mathrm{i}\Delta S_\varepsilon(q, p, t)/\hbar). \tag{5}$$

If in particular, $\{\psi_i\}_{i=0}^{n_r}$ is some complete set, the Wigner function of an incoherent sum of such a set is a constant. We then get

$$\overline{O_{\mathrm{DR}}(t)} = \frac{1}{\mathcal{V}} \int \mathrm{d}q\, \mathrm{d}p \exp(-\mathrm{i}\Delta S_\varepsilon(q, p, t)/\hbar), \tag{6}$$

where $\mathcal{V}$ is the volume of phase space. This expression was used in [25] to compute the FA averaged over initial states. Henceforth, we take $\mathcal{V} = 1$.

Equation (6) is the starting point of our studies. By making some additional assumptions on the dynamics and/or the perturbation, we shall be able to derive analytical expressions for the decay rate of the average FA (the next sections). Being at the basis of our future developments, it is necessary to be sure that (6) gives indeed an accurate description of the FA decay. The DR has successfully passed many tests in the last few years [8, 21, 26], especially in quantum chemistry [27–30]. There has been a similar approach to the DR in the case of linear response functions for electronic spectra [31]. We want, however, to verify its performance in the specific systems that shall be used in this paper.

For the numerical comparisons we have preferred to use quantum maps on the torus. These maps possess all the essential ingredients of the chaotic dynamics and are, at the same time, extremely simple from a numerical point view—both at the classical and at the quantum levels. The periodic boundary conditions that the torus geometry imposes translates in a discretization of both q and p upon quantization. The Hilbert space is then finite dimensional (dimension N) corresponding to an adimensional Planck's constant $\hbar = 1/(2\pi N)$ (we assume the torus has

unit area). Position and momentum basis are related by the discrete Fourier transform (DFT). In such a setting the quantum map corresponds to a unitary operator U [32]. In particular, we choose quantum maps that can be represented in the split-operator form:

$$U = \mathrm{e}^{-\mathrm{i}2\pi NT(\hat{p})}\,\mathrm{e}^{-\mathrm{i}2\pi NV(\hat{q})}. \tag{7}$$

The reason for using maps with this structure is twofold: (i) many well-known classical maps fall in this category, e.g. the standard map, the kicked Harper map, the sawtooth map, as well as some cat maps [32, 33]. (ii) They allow a very efficient numerical implementation due to the possibility of using the DFT.

The classical version of U is

$$\left.\begin{aligned}\bar{p} &= p - \tfrac{\mathrm{d}V(q)}{\mathrm{d}q}\\ \bar{q} &= q + \tfrac{\mathrm{d}T(\bar{p})}{\mathrm{d}\bar{p}}\end{aligned}\right\} \quad (\mathrm{mod}1). \tag{8}$$

Here we shall consider the perturbed cat maps given by [34]

$$\left.\begin{aligned}\bar{p} &= p - a\,q + Kf(q)\\ \bar{q} &= q - b\bar{p} + \tilde{K}h(\bar{p})\end{aligned}\right\} \quad (\mathrm{mod}1). \tag{9}$$

In particular, for the numerics in this section and in section 3, we consider the perturbing 'forces'

$$f(q) = 2\pi\,[\cos(2\pi q) - \cos(4\pi q)]\,, \tag{10}$$

$$h(\bar{p}) = 0. \tag{11}$$

In equation (9) we set $K \ll 1$ and a, b such that the resulting map is completely chaotic (hyperbolic). In such a case the Lyapunov exponent is approximately

$$\lambda \approx \log \frac{1 + ab + \sqrt{ab(4+ab)}}{2}. \tag{12}$$

Time is discrete in maps, so from now on we use the integer n to count time steps. We shall use the K dependence of the quantum map U to define the FA as

$$O(n) = \langle\psi_0|(U_{K'}^{\dagger})^n U_K^n|\psi_0\rangle. \tag{13}$$

Accordingly, the perturbation strength is given by

$$\varepsilon = |K - K'|. \tag{14}$$

In order to calculate the semiclassical DR expression for the average FA, we define an $n_\mathrm{s} = n_q \times n_p$ grid of initial positions and momenta. Thus, we get

$$\overline{O_{\mathrm{DR}}(n)} = \frac{1}{\Omega}\sum_{q,p}\exp[-\mathrm{i}2\pi N\Delta S_\varepsilon(q,\,p,\,n)], \tag{15}$$

where $q = i/n_q$, $p = j/n_p$ (with $i = 0, \ldots, n_q - 1$, $j = 0, \ldots, n_p - 1$) and $\Omega = 1/n_q n_p$. The action difference is

$$\Delta S_\varepsilon(q,\,p,\,n) = -\varepsilon\sum_{i=1}^{n} F(q_i) \tag{16}$$

with $F(q) = \int f(q)\mathrm{d}q$ and the points $(q_i,\,p_i)$ are the successive iterates of the classical map of equation (9).

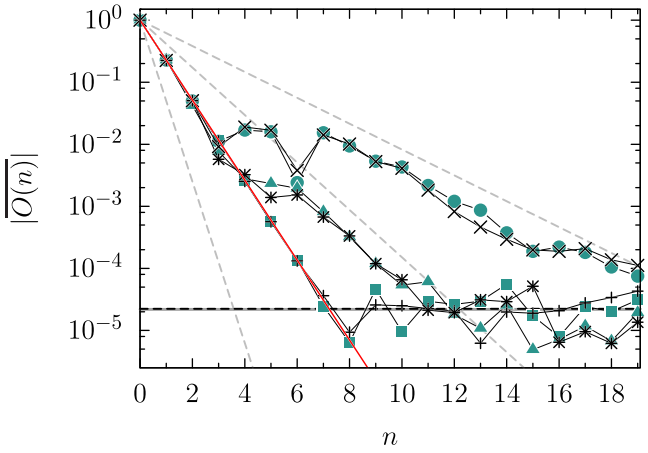

Figure 1. Average FA as a function of time for the perturbed cat map of equation (9) for $a = b = 1$ ($\lambda = 0.96$; • and $\times$), $a = b = 2$ ($\lambda = 1.76$; ▲ and $*$) and $a = b = 20$ ($\lambda = 5.99$; ■ and +). Both $\times$, $*$, and + symbols correspond to the semiclassical approximation (DR) while •, ▲ and ■ correspond to full quantum evolution. The three dashed (grey) lines represent the exponential decay $\exp(-\lambda t/2)$. The solid (red) line is $\exp(-\Gamma t)$ with Γ computed semiclassically (see section 3). We set $\varepsilon/\hbar = 6.433$ which corresponds to $\Gamma = 1.484$. The horizontal lines indicate saturation values: dashed (black) line is $1/\sqrt{n_s}$, with $n_s = 2 \times 10^9$ (DR); solid (grey) line is $1/\sqrt{N \times n_r}$ with $N = 2^{18}$ (Hilbert space dimension) and $n_r = 8000$ (number of initial states).

In figure 1 we show the time evolution of the FA, comparing the semiclassical approximation (DR) with the full quantum evolution. Three perturbed cat maps were considered (with Lyapunov exponents $\lambda = 0.96$, 1.76 and 5.99) under the same perturbation. For the full quantum calculation, we used a dimension $N = 2^{18}$ and averaged over $n_r = 8000$ initial coherent states. For the DR simulation the integral (6) was discretized, the total number of initial conditions being $n_s = 2 \times 10^9$.

We see that the agreement between quantum and semiclassical calculations is quite good in both cases. This makes us confident of the DR as a starting point for the analytical understanding of the average FA. In the next sections, we shall describe two models that explain satisfactorily the main features observed in figure 1: for a large Lyapunov exponent the dynamics can be considered as being essentially random and the decay is single exponential with a rate that depends only on the perturbation (section 3). If the Lyapunov exponent is small and/or the perturbation is large enough the asymptotic decay rate is independent of the perturbation, equal to half the Lyapunov exponent (section 4).

To conclude this section we briefly address the matter of saturation values. The average of n_s, modulo one, complex numbers with uniform random phases goes like $1/\sqrt{n_s}$. Therefore for chaotic systems and long enough times, the DR yields approximately $\overline{O_{DR}(t)} \sim 1/\sqrt{n_s}$. On the other hand, it is well known [35] that the saturation value of equation (13) is determined by $1/\sqrt{N}$, with N being the size of the Hilbert space. Therefore, in the full quantum simulation the saturation value is $\sqrt{N \times n_r}$. Note that in the simulations we chose n_s, n_r, N so that the saturation values of both quantum and semiclassical calculations approximately coincide.

3. Fidelity amplitude for random dynamics

Recently [36] the DR was used to derive analytically the decay rate of the FA for perturbations acting on a small portion of phase space. The advantage of using local perturbations is that we can suppose that the trajectory becomes uncorrelated between successive hits to the perturbed region. It can be argued that the same effect can be achieved for non-local perturbations provided that λ is very large [22].

In this section we study the behaviour of $\overline{O_{\rm DR}}(n)$ in the $\lambda \to \infty$ limit by assuming that the dynamics is purely random. This evolution is completely stochastic in the sense that there is no correlation for the different times of the evolution. To compute $\overline{O_{\rm DR}}(n)$, we make a partition of the phase space in N_c cells. We consider that the probability to jump from one cell to any other in phase space is uniform. Therefore it is straightforward to show that the mean FA results in

$$\begin{aligned}\overline{O_{\rm DR}}(n) &= \frac{1}{N_c^n}\sum_{j_1}\ldots\sum_{j_n}\exp[-{\rm i}(\Delta S_{\varepsilon,j_1}+\cdots+\Delta S_{\varepsilon,j_n})/\hbar] \\ &= \left[\frac{1}{N_c}\sum_{j}\exp\left(-{\rm i}\Delta S_{\varepsilon,j}/\hbar\right)\right]^n, \end{aligned} \tag{17}$$

where $\Delta S_{\varepsilon,j_k}$ is the action difference evaluated in the cell j_k at time k. The continuous limit is approached when $N_c \to \infty$. So, $\overline{O_{\rm DR}}(n)$ results in

$$\overline{O_{\rm DR}}(n) = \left(\int \exp\left[-{\rm i}\Delta S_\varepsilon(q,\,p)/\hbar\right]{\rm d}q\,{\rm d}p\right)^n, \tag{18}$$

where $\Delta S_\varepsilon(q,\,p)$ is the action difference after one step of the map. This exponential decay can be rewritten as

$$\overline{O_{\rm DR}}(n) = \exp(-\Gamma\, n), \tag{19}$$

with

$$\Gamma = -\log\left|\int \exp[-{\rm i}\Delta S_\varepsilon(q,\,p)/\hbar]{\rm d}q\,{\rm d}p\right|. \tag{20}$$

Equation (20) is one of the key results of this work: if the dynamics is (uncorrelated) random, then the average FA decays exponentially with decay rate Γ. In figure 2, we plot Γ as a function of the rescaled perturbation strength $\varepsilon/\hbar$ for the map of equation (9). The circles mark the perturbation strength values used in figures 1 and 3.

In both figures 1 and 3 the agreement with the random-dynamics approach is well observed for initial times.

If λ is large enough ($\lambda = 5.99$ for ■ and + symbols in figures 1 and 3), the dynamics can be considered as random for practical purposes and the decay rate—up to saturation—is given by Γ.

In section 4 we shall see in a specific deterministic model (the baker family) how a large Lyapunov exponent leads to an effective decorrelation of the successive points in a trajectory and therefore the map behaves as if it were random.

We point out that in figures 1 and 3, after the initial decay following the random dynamics predictions, there is a crossover to a different decay rate. In figure 1, the second decay rate is $\lambda/2$, while in figure 3 it is not. In sections 4 and 5 we analyse this crossover behaviour in more detail.

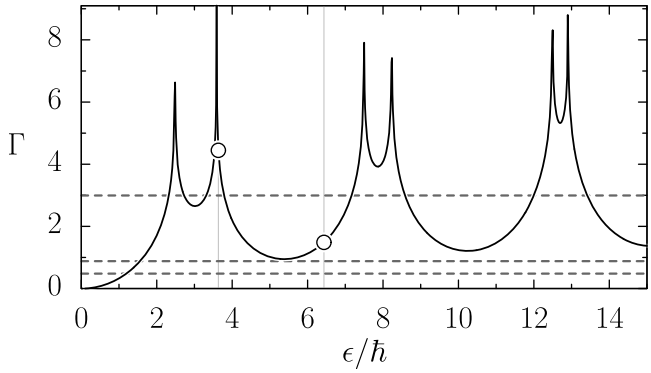

Figure 2. Decay rate Γ computed from equations (19) and (20) as a function of the rescaled perturbation. The points indicate the values chosen in figure 1 ($\varepsilon/\hbar = 6.433$) and figure 3 ($\varepsilon/\hbar = 3.635$). The dashed horizontal lines are the corresponding $\lambda/2$ used in figure 1 (0.96/2, 1.76/2 and 5.99/2).

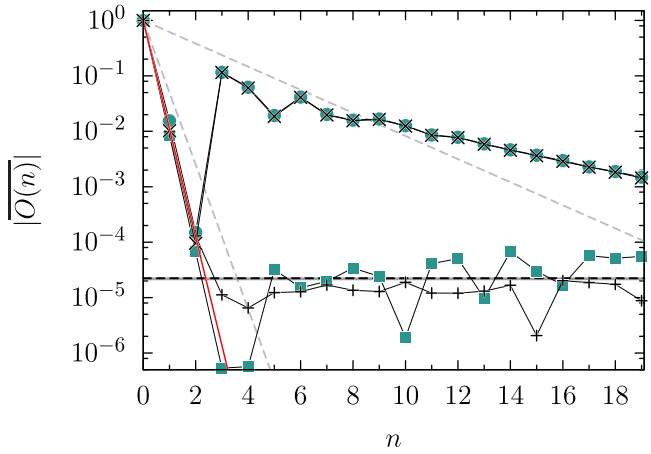

Figure 3. The same as figure 1 with $\varepsilon/\hbar = 3.635$ corresponding to $\Gamma = 4.448$.

4. The random-perturbation limit

In the previous section, we showed that a large Lyapunov exponent leads to a decay that is well described by the random dynamical model. Here we argue that for large-enough perturbations a Lyapunov decay must be expected.

Key to our analysis is the implementation of the transfer matrix method of calculating the semiclassical average FA. The transfer matrix method is a standard tool in statistical mechanics for the calculation of the partition function of Ising lattices [37–39]. Due to the analogy between Ising partition functions (for imaginary temperature) and semiclassical periodic orbit sums, the method has also found applications in the quantum chaos domain [40–43].

We start by analysing the particularly simple case of the baker map and a random perturbation. Then, we provide analytical and numerical evidence showing that such a Lyapunov decay should also be observed in a larger class of chaotic maps subjected to non-random (large enough) perturbations.

4.1. The baker map and the transfer matrix method

The baker's transformation is an area-preserving, piecewise-linear map of the unit square defined by [44]

$$q_1 = 2q_0 - \mu_0, \tag{21}$$

$$p_1 = (p_0 + \mu_0)/2, \tag{22}$$

where $\mu_0 = [2q_0]$, the integer part of $2q_0$. This map admits a very useful description in terms of a complete symbolic dynamics [45]. A one to one correspondence between phase space coordinates and binary sequences,

$$(p, q) \leftrightarrow \ldots \mu_{-2}\mu_{-1} \cdot \mu_0\mu_1\mu_2 \ldots, \quad \mu_i = 0, 1, \tag{23}$$

can be constructed in such a way that the action of the map is conjugated to a shift map. The symbols are assigned as follows: μ_i is set to zero (one) when the ith iteration of (p, q) falls to the left (right) of the line $q = 1/2$, i.e. $[2q_i] = \mu_i$. Reciprocally, given an itinerary $\ldots \mu_{-2}\mu_{-1} \cdot \mu_0\mu_1\mu_2 \ldots$, the related phase point is obtained through the especially simple binary expansions

$$q = \sum_{i=0}^{\infty} \frac{\mu_i}{2^{i+1}} \equiv .\mu_0\mu_1 \ldots, \tag{24}$$

$$p = \sum_{i=1}^{\infty} \frac{\mu_{-i}}{2^i} \equiv .\mu_{-1}\mu_{-2} \ldots. \tag{25}$$

For simplicity, let us initially consider a perturbation that depends only on q. Using the binary expansions defined above, the DR average FA (15) and (16) reads

$$\overline{O_{\mathrm{DR}}(n)} = \int_0^1 \mathrm{d}q_0 \, \mathrm{e}^{\mathrm{i}\varepsilon\left[F(.\mu_0\mu_1\mu_2\ldots)+F(.\mu_1\mu_2\mu_3\ldots)+\cdots+F(.\mu_{n-1}\mu_n\mu_{n+1}\ldots)\right]}. \tag{26}$$

Here and in the rest of this section, for the sake of a lighter notation, we write just ε in place of $\varepsilon/\hbar$.

In order to introduce the transfer matrix method it is necessary to truncate the binary expansions at a finite length L, i.e.

$$q \approx \sum_{i=0}^{L-1} \frac{\mu_i}{2^{i+1}}. \tag{27}$$

Equivalently one may think that we are treating exactly a perturbation that is constant over vertical strips of equal width $1/2^L$ (we adopt this point of view). With this proviso the integral (26) becomes a finite sum:

$$\overline{O_{\mathrm{DR}}(n)} = 2^{-(n+L-1)} \sum_{\mu_0,\ldots,\mu_{n+L-2}=0,1} \mathrm{e}^{\mathrm{i}\varepsilon\left[F(.\mu_0\ldots\mu_{L-1})+F(.\mu_1\ldots\mu_L)+\cdots+F(.\mu_{n-1}\ldots\mu_{n+L-2})\right]}. \tag{28}$$

The prefactor $2^{-(n+L-1)}$ represents the *area* (weight, probability) of the region in phase space corresponding to the finite symbolic string $\mu_0, \ldots, \mu_{n+L-2}$ (the area depends on the length only, not on the particular code). These regions taken together form a partition of phase space into disjoint elements. All the trajectories starting in a given element have the same action.

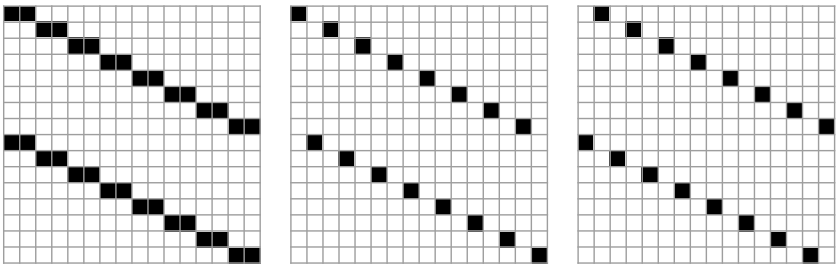

Figure 4. The transfer matrix M (left) can be split into two unitary matrices U_1, U_2 (centre, right). Nonzero elements are shown as black squares ($L = 5$, schematic).

The trick now is to express the sum above as a product of n matrices. Define the indices

$$k_0 = 2^{L-1} \times .\mu_0 \dots \mu_{L-2}, \tag{29}$$

$$k_1 = 2^{L-1} \times .\mu_1 \dots \mu_{L-1}, \tag{30}$$

$$\dots = \dots, \tag{31}$$

$$k_n = 2^{L-1} \times .\mu_n \dots \mu_{L+n-2}. \tag{32}$$

Then we can write

$$\overline{O_{\mathrm{DR}}(n)} = 2^{-(n/2+L-1)} \sum_{k_0,\dots,k_n} M_{k_0,k_1} M_{k_1,k_2} \dots M_{k_{n-1},k_n}, \tag{33}$$

where the non-zero elements of the matrix M are given by

$$M_{k_0,k_1} = \frac{1}{\sqrt{2}} \mathrm{e}^{\mathrm{i}\varepsilon F(.\mu_0 \dots \mu_{L-1})} \tag{34}$$

(the convenience of having introduced a factor $\sqrt{2}$ will become clear soon). It is implicit in this definition that k_0 and k_1 must satisfy the *shift condition*, i.e. they must share the bits $\mu_1 \dots \mu_{L-2}$ (see equations (29) and (30)), otherwise the matrix element is set to zero. The shift condition determines that non-zero elements are located on two staircases of slope 1/2 ('baker structure'), explicitly given by

$$k_1 = 2k_0 - 2^{L-1}\mu_0 + \mu_{L-2} \tag{35}$$

(see figure 4).

If one defines the unit-norm vector

$$|1\rangle = \frac{1}{\sqrt{2^{L-1}}}(1, 1, \dots, 1), \tag{36}$$

then equation (33) can be written in the compact way

$$\overline{O_{\mathrm{DR}}(n)} = 2^{-n/2} \langle 1| M^n |1\rangle. \tag{37}$$

This is a remarkable result: the decay properties of the average FA are embodied in the spectrum of a finite matrix. In particular, the asymptotic decay is ruled by the largest eigenvalue (in modulus) of M. The special staircase structure of the transfer matrix allows us to deduce some general properties of its spectrum.

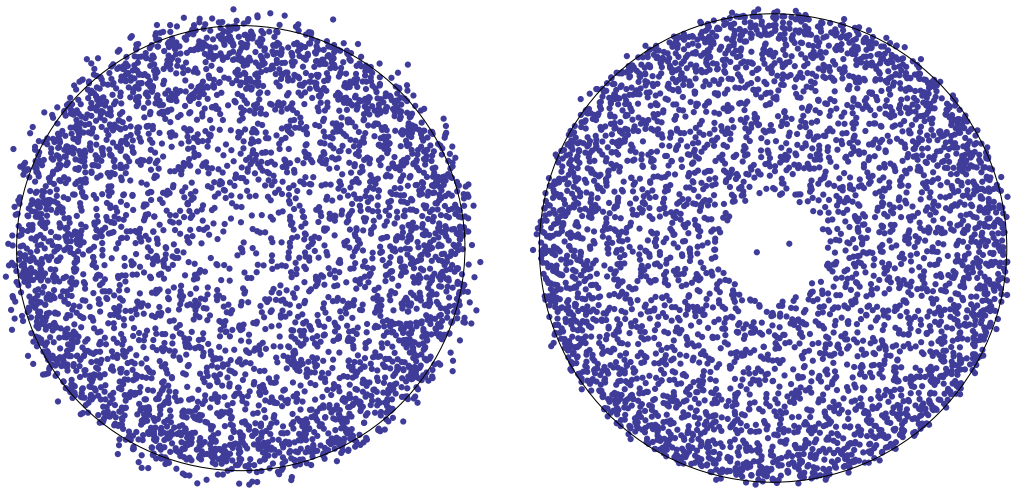

Figure 5. Eigenvalues z_i of random matrices having the baker structure. Shown are the combined spectra of 64/8 matrices of dimension $64 \times 64/512 \times 512$ (left/right). Circles of unit radii are drawn for reference.

For a fine discretization, the phase in equation (34) varies by small jumps along the staircases of M, the size of the jumps depending both on the characteristic spatial scale of $F(q)$ ('correlation length') and on the perturbation amplitude ε. As the correlation length decreases and/or the amplitude grows, neighbouring matrix elements become increasingly decorrelated. This leads us to consider, as a reference, an ensemble of random transfer matrices having the same structure as M, but whose phases are i.i.d. random variables chosen from a uniform distribution in $[0, 2\pi]$.

Random or not, because of its particular structure, the matrix M can be split as a sum of two unitary matrices U_1, U_2 (see figure 4):

$$M = \frac{1}{\sqrt{2}} (U_1 + U_2) . \tag{38}$$

When U_1 and U_2 are random unitary matrices drawn independently from the circular unitary ensemble (CUE) [32, 46], analytical and numerical studies tell that the spectrum of M lies almost entirely inside the unit circle in the complex plane. As the dimension of U_i is increased, the largest eigenvalue (in modulus) tends to the unit circle. In the limit of infinite dimensional matrices, all the spectrum is contained in the unit disc [43, 47].

We have not attempted an analytical study of the spectral properties of random matrices with the baker structure. However, our numerical calculations show that they possess very similar statistical properties to those of the normalized sum of two CUE matrices (as far as the spectrum close to the unit circle is concerned). Figure 5 shows clearly that most eigenvalues are distributed inside the unit circle, the relative number of 'outsiders' decreasing as the dimension in increased.

So, as the leading eigenvalues of M are close to the unit circle, we conclude that for a random perturbation the asymptotic decay of $\overline{O_{\mathrm{DR}}(n)}$ is governed by the prefactor in (37); thus we have

$$|\overline{O_{\mathrm{DR}}(n)}|^2 \sim 2^{-n}. \tag{39}$$

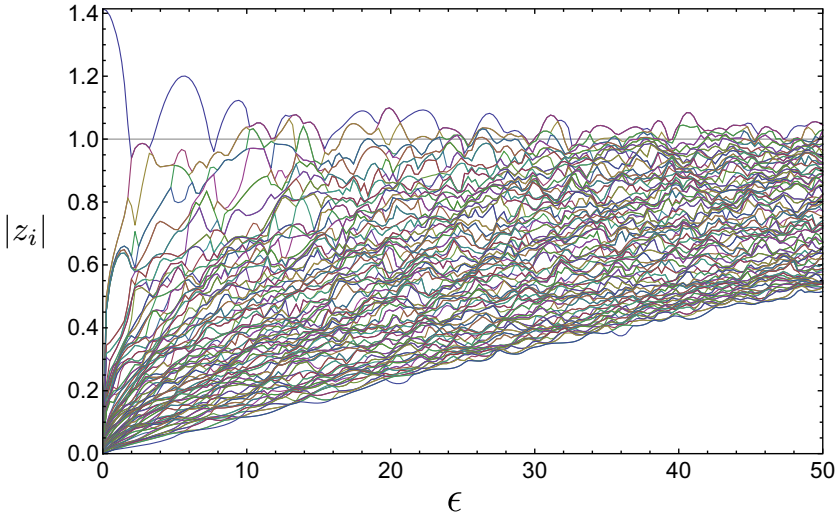

Figure 6. Transfer matrix eigenvalues (moduli) as a function of perturbation amplitude. The perturbation $F(q) = \sin(2\pi q) - \sin(4\pi q)/2$ was discretized in a lattice of 256 points ($L = 7$).

This is an exponential decay, with a rate given by the Lyapunov exponent of the baker map. This is the other key result of the present work: starting from the FA and using the DR and the transfer matrix method, we obtain that the asymptotic decay of the average FA is given by $\lambda/2$ (consequently the fidelity decays with the rate lambda).

After having analysed the random transfer-matrix model, we ask to what extent a non-random perturbation may lead to a random-matrix behaviour. As mentioned before, e.g. a smooth but large perturbation may cause a randomization of the phases (34). In order to check this expectation we consider now the baker dynamics with the action difference of equations (16) and (10), i.e. $F(q) = \sin(2\pi q) - \sin(4\pi q)/2$. The spectrum of the corresponding $M(\varepsilon)$ is shown in figure 6.

There we see that for, say, $\varepsilon > 10$ the leading eigenvalues settle down in a small neighbourhood of the unit circle. Then, for such large perturbations $|\overline{O_{\mathrm{DR}}(n)}|^2$ decays with a rate that is close to the Lyapunov exponent of the classical map.

Note, however, that in typical numerical simulations the decay rate may exhibit some departure from the Lyapunov exponent. This may be due to two reasons. Firstly, the perturbation amplitude may be not large enough for the settling down of the Lyapunov regime. Secondly, even for completely random perturbations, if M is finite dimensional, then the leading eigenvalue will be in general outside the unit circle. It is true that as the dimension N of M is increased, the leading eigenvalue tends to the unit circle, but it does so very slowly, possibly like $N^{-1/3}$ [43]. So, in practice, some finite deviations from the Lyapunov decay rate should not be ruled out.

4.2. Extensions

Here we present some extensions of the application of the transfer matrix method to account for more general maps and/or perturbations.

First note that perturbations that depend both on q and p can easily be accommodated in the transfer-matrix scheme for, according to (23), it requires only adding some symbols for the discretization in p.

Now consider the B-adic baker map defined by (see [48])

$$q_1 = Bq_0 - \nu_0, \tag{40}$$

$$p_1 = (p_0 + \nu_0)/B, \tag{41}$$

where B is an integer $\geqslant 2$, and $\nu = 0, 1, \ldots, B-1$. This map is completely analogous to the usual ($B = 2$) baker map, but with expansion rate B. At the symbolic level it corresponds to a full shift on B symbols [45]. Its Lyapunov exponent is $\log B$. Thus, by making B large enough we shall be able to enter the random-dynamics regime (section 3).

The transfer matrix M is constructed in a similar way as we did for the baker: basically, all we have to do is to change from base-2 to base-B in the standard-baker formulae. By making the appropriate substitutions and skipping the details, one arrives at the following expression for the average FA:

$$\overline{O_B(n)} = B^{-n/2} \langle 1 | M_B^n | 1 \rangle, \tag{42}$$

with $|1\rangle$ being a unit-norm vector of length B^{L-1}.

For a perturbation that only depends on q the non-null elements of M_B read

$$(M_B)_{k_0,k_1} = \frac{1}{\sqrt{B}} \mathrm{e}^{\mathrm{i}\varepsilon F(\nu_0 \ldots \nu_{L-1})}, \tag{43}$$

where ν_i are the 'decimal' digits of the B-ary expansion of the coordinate q, truncated at depth L. The non-null elements of M_B lie along B flights of stairs of slope $1/B$ (riser $= 1$, tread $= B$). In analogy to the $B = 2$ case, we can split M_B into a sum of unitary matrices:

$$M_B = \frac{1}{\sqrt{B}} \sum_{i=1}^{B} U_i. \tag{44}$$

Again, in the case when U_i are large independent CUE matrices, it is possible to show that the spectrum of M_B is almost completely contained in the unit disc in the complex plane [47]. The same behaviour is expected for the transfer matrix of the baker family when a non-random but large enough perturbation is considered. In such a case, one would have the asymptotic decay

$$|\overline{O_B(n)}| \sim \mathrm{e}^{-\lambda_B n/2}, \tag{45}$$

with $\lambda_B = \log B$, the Lyapunov exponent of the classical B-baker map. As an example, we show in figure 7 the transfer matrix spectrum for $B = 13$ and a smooth perturbation.

Plotted are the decay rates

$$\gamma_i = \frac{\log B}{2} - \log |z_i|, \tag{46}$$

where $\{z_i\}$ stand for the eigenvalues of M_B.

Focusing on the asymptotic decay, we see that for small perturbation amplitudes the decay is very well described by the random-dynamics model, as was expected from the discussion of

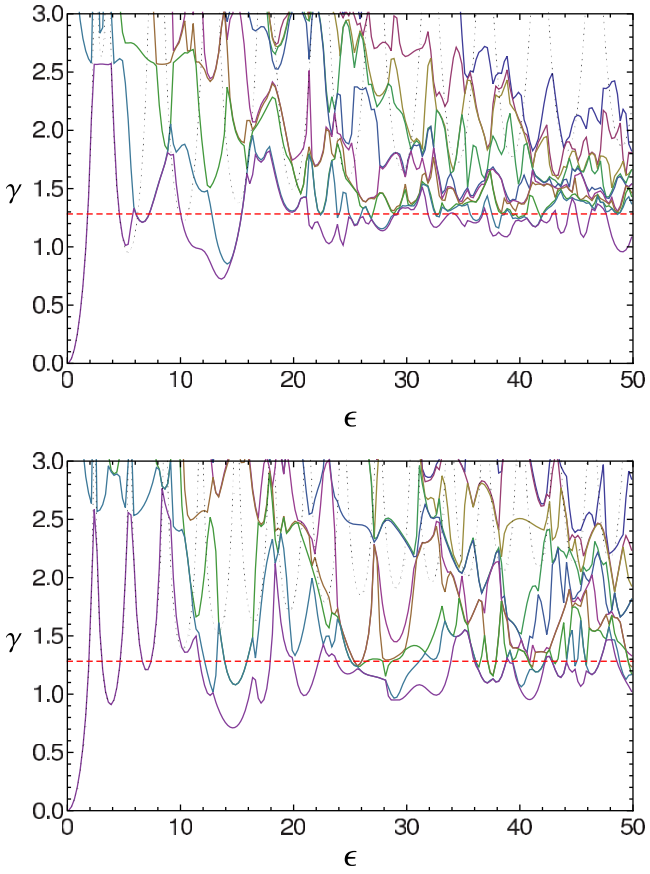

Figure 7. Transfer matrix decay rates for the $B = 13$ baker as a function of perturbation amplitude. We considered two perturbed actions $F(q) = \sin(2\pi q) - \sin(4\pi q)/2$ (top panel) and $F(q) = \sin(2\pi q)$ (bottom panel). These functions were discretized in a lattice of 2197 points ($L = 3$). Dashed horizontal lines correspond to Lyapunov decay, i.e. $(\log B)/2$. Dotted lines are the predictions of the random-dynamics model.

section 3. Note, however, that the extension of the random-dynamic regime is sensitive to the *form* of the perturbation. For large ε the leading decay rate fluctuates around the Lyapunov value $(\log B)/2$, in a similar way as we saw in the case of the standard baker.

The baker family permits a transparent estimation of the crossover point between random-dynamics and Lyapunov regimes. For a q-dependent perturbation and a B-baker map, the average FA is given by

$$\overline{O_{\mathrm{DR}}(n)} = \int_0^1 \mathrm{d}q_0\, \mathrm{e}^{\mathrm{i}\varepsilon\left[F(q_0)+F(q_1)+\cdots+F(q_{n-1})\right]}. \tag{47}$$

Here it is implicit that $q_1, q_2, \ldots$ are related to q_0 by the dynamics. Alternatively we can take q_i to be independent and write

$$\overline{O_{\mathrm{DR}}(n)} = \int \mathrm{d}q_0\, \mathrm{d}q_1\, \ldots \mathrm{d}q_{n-1}\, \mathrm{e}^{\mathrm{i}\varepsilon\left[F(q_0)+F(q_1)+\cdots F(q_{n-1})\right]} P(q_0, q_1, \ldots, q_{n-1}), \tag{48}$$

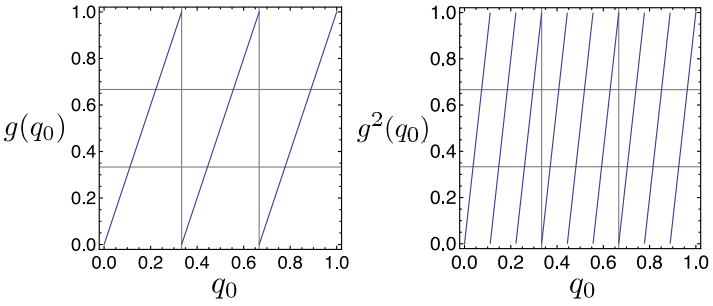

Figure 8. The probability distribution is a product of delta functions $\delta(q_1 - g(q_0))\delta(q_2 - g^2(q_0))\ldots$. Gridlines define the critical square binning. All bins contain the same probability, meaning that the histogram is constant, therefore separable. The same is true for any bin size larger than $1/B$ ($B = 3$ in these plots).

where

$$P(\ldots) = \delta(q_1 - g(q_0))\delta(q_2 - g^2(q_0))\ldots\delta(q_{n-1} - g^{n-1}(q_0)), \tag{49}$$

and $g(q) = Bq - [Bq]$.

If the joint probability distribution P were factorable, then we would recover the formula for random dynamics. Strictly speaking this factorization is impossible for a deterministic dynamics; however, when considering P in the context of the integral above, one sees that P admits some coarse graining without affecting the integral. This is true whenever the scale for the smoothing is smaller than the typical scale of variation of the phase $\exp(\mathrm{i}\varepsilon\ldots)$, which is of the order of $1/\varepsilon$. The smaller the ε, the larger the smoothing of P we are allowed to do. Suppose that the smoothing consists of substituting P by a histogram of bin size $a \sim 1/\varepsilon$ for each coordinate (see figure 8). Then, by choosing $a \geqslant 1/B$ the smoothed distribution becomes a constant, i.e. becomes separable (the marginals are constant).

We conclude that for $\varepsilon \lesssim B$ the distribution P is *effectively* separable and the random-dynamic result is applicable.

Concerning the application of the transfer matrix method to more general maps with a finite symbolic dynamics, e.g. cat maps, it is likely that the scheme can also be adapted to this case.

The general structure of the transfer matrix will be the same as that of the corresponding baker with the same number of symbols. The novelty is that some zeros will appear along the staircases whenever the associated symbolic sequence is prohibited (the information about allowed and prohibited sequences is contained in the transition matrix [45]). The correspondence between symbols and phase space points will be non-trivial, but it could be settled numerically, just by launching initial conditions and registering the sequence of Markov regions that are visited.

The main obstacle we see at the moment is that in general the symbolic sequences do not have the same weight. It is possible that these weights can be embodied in the transfer matrix, or it may be a good approximation to assume that for long sequences the weights are equal. This issue, which exceeds the original scope of the present paper, is currently being investigated [49].

5. The crossover regime

In the previous sections, we provided analytical descriptions of the FA in two extreme cases: the random dynamics limit and the random perturbation limit. The first model provides a satisfactory description for initial times in general and for all times—before saturation—in the large λ limit (ideally $\lambda \to \infty$). The second explains the appearance of the Lyapunov regime for long times and large enough perturbations.

In many cases the time behaviour of the FA is not pure, but shows a crossover from a random-dynamics decay (short times) to a random-perturbation decay (long times). We know that for short times the influence of the dynamics is not significant on average, then the trajectories in the DR formula (15) behave like random walks with uncorrelated jumps. Therefore, for short times the decay of the average FA is given by equation (20)—it is exact for $t = 1$. In addition, for a general smooth perturbation with large amplitude, we have shown that there is a randomization of phases yielding an effectively random perturbation. As a consequence, the well-known Lyapunov decay emerges in the large ϵ limit. There remains a need for understanding the crossover (in the time domain) between random-dynamics and Lyapunov decays.

In order to investigate the crossover we resorted to numerical simulations using the DR and the cat map (9) with a random perturbation. We divided the torus into $N_c \times N_c$ square cells, assigning a random constant value $v_i \in [-0.5, 0.5]$ to each cell, with $i \in [1, N_c^2]$. Next we computed $\overline{O_{\mathrm{DR}}(n)}$ by summing over n_{s} initial conditions and then averaged $|\overline{O_{\mathrm{DR}}(n)}|$ over N_{rc} realizations of the perturbation.

In figure 9 we show the results of our simulations for various values of ϵ and λ. Using equations (19) and (20) we computed the decay rate Γ for the initial times (see the inset). We can already see on the top panel that $\langle|\overline{O_{\mathrm{DR}}(n)}|\rangle$ has three well-defined regimes: two exponential decays followed by the expected saturation due to a finite number of initial conditions. Then, up to the saturation point, the decay is well described by

$$\langle|\overline{O_{\mathrm{DR}}(n)}|\rangle \sim \exp(-\Gamma n) + A\exp(-\lambda n/2). \tag{50}$$

We found empirically that, in our particular model, the prefactor A is given by

$$A = \lambda/N_c. \tag{51}$$

So, when $\lambda \to \infty$ the dynamics is random, the second term vanishes, and the decay rate is Γ for all times before saturation, as predicted in section 3. When λ is finite but the perturbation is completely random ($N_c \to \infty$) the first term in equation (50) dominates the initial decay. The reason for this is that deterministic motion together with random perturbations, on short time scales, like random dynamics (as far as the accumulation of phases is concerned).

In figure 9 (the top and middle panels), the dependence of A on λ is clearly observed. The dependence on N_c is established in the bottom panel, where we plot $\langle|\overline{O_{\mathrm{DR}}(n)}|\rangle$ for three different orders of magnitude of the randomness parameter N_c. We remark that, as expected, the crossover point depends both on the dynamics (through λ) and on the perturbation (through N_c). We can clearly see this in the middle panel of figure 9 where we show $\langle|\overline{O_{\mathrm{DR}}(n)}|\rangle$ for different values of the rescaled perturbation strength $\epsilon/\hbar$ (and for $\lambda = 0.96$, corresponding to $a = b = 1$ in equation (9)) and in the bottom panel of the same figure where we plot $\langle|\overline{O_{\mathrm{DR}}(n)}|\rangle$ for one value of $\epsilon/\hbar$ and $N_c = 10,\ 100$ and 1000. We can again see that equation (50) describes quite well the decay up to the saturation value.

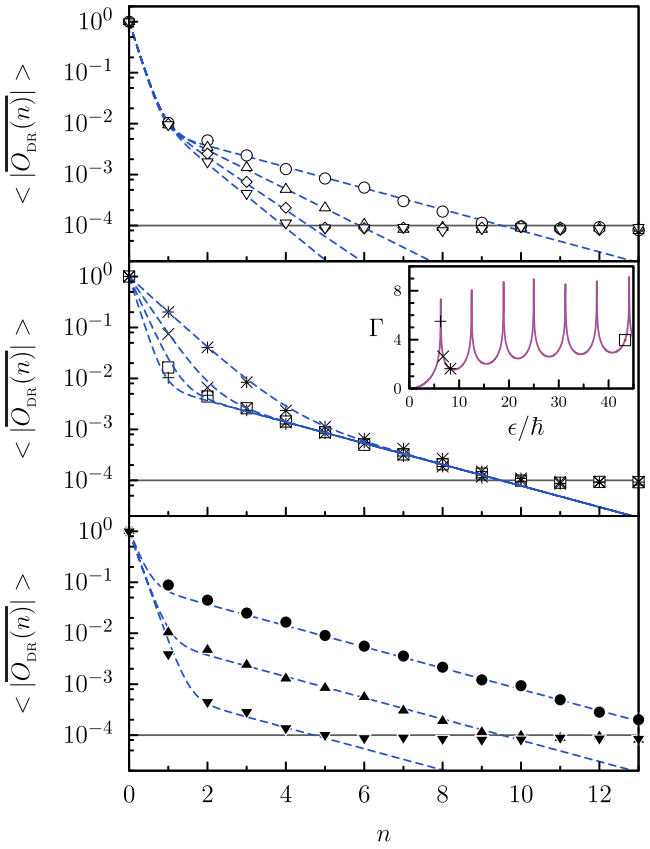

Figure 9. Top: $\langle|\overline{O_{\rm DR}(n)}|\rangle$ for $\epsilon/\hbar = 6.2589$ (+ symbol in the inset) and different values $a = b = 1,\ 2,\ 3$ and 4 in equation (9) giving ($\circ$) $\lambda = 0.96$, ($\triangle$) $\lambda = 1.76$, ($\diamond$) $\lambda = 2.389$ and ($\triangledown$) $\lambda = 2.887$, respectively. Middle: $\langle|\overline{O_{\rm DR}(n)}|\rangle$ for $a = b = 1$, $\lambda = 0.96$ and different perturbation strengths: (+) $\epsilon/\hbar = 6.2589$; ($\times$) $\epsilon/\hbar = 6.794$; ($*$) $\epsilon/\hbar = 8.235$; ($\square$) $\epsilon/\hbar = 43.318$. Inset: $\Gamma(t)$ computed from $N_{\rm rc} = 100$ realizations of the perturbation with $N_c = 100$. The points indicate the value of $\epsilon/\hbar$ for the curve with the corresponding symbol on the bottom panel. Bottom: $\langle|\overline{O_{\rm DR}(n)}|\rangle$ for $\epsilon/\hbar = 6.2589$ (+ symbol in the inset), for three different values of N_c: ($\bullet$) $N_c = 10$, ($\blacktriangle$) $N_c = 100$ and ($\blacktriangledown$) $N_c = 1000$ ($a = b = 1$, $\lambda = 0.96$). The dashed blue line (in all panels) corresponds to the bi-exponential in equation (50). The horizontal gray lines correspond to the expected saturation values.

We thus verify that the crossover regime can be described by a natural bi-exponential law combining the random-dynamic and Lyapunov decays.

6. Conclusions

We have analysed the average FA, a quantity that characterizes the instability and irreversibility of perturbed quantum evolution. We have taken as a starting point a well-established semiclassical theory—the DR. Our first key result is obtained in the limit of random dynamics. We show that in that case the decay of the average FA is exponential for all times—up to the

saturation—and we give an analytic expression for the corresponding decay rate. Maps on the torus with a very large Lyapunov exponent are expected to mimic random dynamics rather precisely. Thus the decay rate Γ obtained in equation (20) is to be observed for increasingly larger periods of time as λ is increased. Numerical results shown in figures 1 and 3 confirm this assertion.

Our second key result is that using the DR and a novel approach in this context—the transfer matrix method—we were able to predict that the asymptotic decay of the average FA should be perturbation independent and given by $\lambda/2$. We are even able to explain possible deviations from this behaviour. We point out that the Lyapunov as well as other regimes were obtained in [19] analysing statistics of action differences in an expression that is obtained from the square of the average FA (equation (6)). However, in that paper the short time behaviour due to random dynamics-like behaviour is not observed. In addition, one major advantage of our approach is that we do not need to sum over pairs of trajectories—a difficulty that arises in the squaring needed to perform average fidelity studies.

As a consequence, we have both analytical and numerical evidence to conclude that the average FA for an arbitrary chaotic map should decay initially with a decay rate given by the random dynamics approximation and for long times there is the Lyapunov regime. We cannot yet predict in a generic case the behaviour or the time where the crossover takes place. Nevertheless, in an attempt to understand this problem we have studied a model of random perturbations that helped us to determine that for random perturbations and intermediate times the decay is also given by the Lyapunov exponent.

In [22] it is shown that the decay of the LE has three regimes as a function of the perturbation strength. The well known—quadratic—Fermi golden rule regime is valid for small perturbations. Then there is a regime where the decay rate is given by Γ (computed for random dynamics) and after that there is a crossover to a perturbation-independent regime given by the Lyapunov exponent λ. We believe that this paper is an important step towards understanding this complex behaviour of the LE. We remark that the average FA is tightly related to the LE but has some fundamental differences. In fact, if we suppose that n_s is the number of initial conditions, then the average LE can be expressed as a sum of the square of the average of the FA (times n_s) minus a sum of 'non-diagonal' terms consisting of products of $O(t)$ for different initial conditions. Here we have taken a significant step forward by understanding one of the parts of the LE: the average FA, which is in itself an important quantity in many experiments. In order to fully comprehend the behaviour of the LE, further work is needed [49].

Acknowledgments

We are grateful to F Toscano for useful suggestions. We received partial support from ANCyPT (grant no. PICT-2010-1556), UBACyT (grant no. X237; Argentina), CNPq (Brazil) and UNAM-PAPIIT (grant no. IN117310; Mexico).

References

[1] Peres A 1984 *Phys. Rev.* A **30** 1610
[2] Jalabert R A and Pastawski H M 2001 *Phys. Rev. Lett.* **86** 2490
[3] Jacquod Ph, Silvestrov P G and Beenakker C W J 2001 *Phys. Rev.* E **64** 055203
[4] Gorin T, Prosen T, Seligman T and Žnidarič M 2006 *Phys. Rep.* **435** 33

[5] Jacquod Ph and Petitjean C 2009 *Adv. Phys.* **58** 67
[6] Prosen T and Žnidarič M 2002 *J. Phys. A: Math. Gen.* **35** 1455
[7] Prosen T 2002 *Phys. Rev.* E **65** 036208
[8] Wang W, Casati G and Li B 2004 *Phys. Rev.* E **69** 025201
[9] Andersen M, Kaplan A, Grünzweig T and Davidson N 2006 *Phys. Rev. Lett.* **97** 104102
[10] Pozzo E N and Domínguez D 2007 *Phys. Rev. Lett.* **98** 057006
[11] Ares N and Wisniacki D A 2009 *Phys. Rev.* E **80** 046216
[12] Casabone B, García-Mata I and Wisniacki D 2010 *Europhys. Lett.* **89** 50009
[13] Lobkis O I and Weaver R L 2003 *Phys. Rev. Lett.* **90** 254302
[14] Schäfer R, Stöckmann H J, Gorin T and Seligman T H 2005 *Phys. Rev. Lett.* **95** 184102
[15] Schäfer R, Gorin T, Seligman T H and Stöckmann H J 2005 *New J. Phys.* **7** 152
[16] Gorin T, Seligman T H and Weaver R L 2006 *Phys. Rev.* E **73** 015202
[17] Lobkis O I and Weaver R L 2008 *Phys. Rev.* E **78** 066212
[18] Köber B, Kuhl U, Stöckmann H J, Gorin T, Savin D V and Seligman T H 2010 *Phys. Rev.* E **82** 036207
[19] Vaníček J 2004 *Phys. Rev.* E **70** 055201
[20] Vaníček J and Heller E J 2003 *Phys. Rev.* E **68** 056208
[21] Vaníček J 2006 *Phys. Rev.* E **73** 046204
[22] García-Mata I and Wisniacki D A 2011 *J. Phys. A: Math. Theor.* **44** 315101
[23] Miller W H 1970 *J. Chem. Phys.* **53** 3578
[24] Miller W H 2001 *J. Phys. Chem* A **105** 2942
[25] Vaníček J 2004 arXiv:quant-ph/0410205
[26] Wang W, Casati G, Li B and Prosen T 2005 *Phys. Rev.* E **71** 037202
[27] Li B, Mollica C and Vaníček J 2009 *J. Chem. Phys.* **131** 041101
[28] Zimmermann T and Vaníček J 2010 *J. Chem. Phys.* **132** 241101
[29] Zimmermann T, Ruppen J, Li B and Vaníček J 2010 *Int. J. Quantum Chem.* **110** 2426
[30] Wehrle M, Šulc M and Vaníček J 2011 *CHIMIA Int. J. Chem.* **65** 334
[31] Shi Q and Geva E 2005 *J. Chem. Phys.* **122** 064506
[32] Haake F 2010 *Quantum Signatures of Chaos* (Berlin: Springer)
[33] de Almeida A M O 1988 (Cambridge: Cambridge University Press)
[34] de Matos M B and de Almeida A M O 1995 *Ann. Phys.* **237** 46
[35] Gutiérrez M and Goussev A 2009 *Phys. Rev.* E **79** 046211
[36] Goussev A, Waltner D, Richter K and Jalabert R A 2008 *New J. Phys.* **10** 093010
[37] Dobson J F 1969 *J. Math. Phys.* **10** 40
[38] Borzi C, Ord G and Percus J K 1987 *J. Stat. Phys.* **46** 51
[39] Reichl L E 1998 *A Modern Course in Statistical Physics* (New York: Wiley)
[40] Gutzwiller M C 1990 *Chaos in Classical and Quantum Mechanics* (New York: Springer)
[41] Kaplan L and Heller E J 1996 *Phys. Rev. Lett.* **76** 1453
[42] Smilansky U and Verdene B 2003 *J. Phys. A: Math. Gen.* **36** 3525
[43] Carlo G G, Vallejos R O and Abreu R F 2010 *Phys. Rev.* E **82** 046220
[44] Arnold V I and Avez A 1989 *Ergodic Problems in Classical Mechanics* (Reading, MA: Addison-Wesley)
[45] Adler R L 1998 *Bull. Am. Math. Soc.* **35** 1
[46] Mehta M L 2004 *Random Matrices* (Amsterdam: Elsevier)
[47] Görlich A and Jarosz A 2004 arXiv:math-ph/0408019
[48] Sano M M 2000 *CHAOS* **10** 195
[49] García-Mata I, Vallejos R O and Wisniacki D A In preparation